Chronology of the Last Climatic Cycle (Upper Pleistocene) of the Surduk loess sequence, Vojvodina, Serbia

MARKUS FUCHS, DENIS-DIDIER ROUSSEAU, PIERRE ANTOINE, CHRISTINE HATTÉ, CAROLINE GAUTHIER, SLOBODAN MARKOVIĆ AND LUDWIG ZOELLER

BOREAS

Fuchs, M., Rousseau, D.-D., Antoine, P., Hatté, C., Gauthier, C., Marković, S. & Zoeller, L. 2008 (February): Chronology of the Last Climatic Cycle (Upper Pleistocene) of the Surduk loess sequence, Vojvodina, Serbia. *Boreas*, Vol. 37, pp. 66–73. 10.1111/j.1502-3885.2007.00012.x. ISSN 0300-9483.

The Surduk loess section in Serbia provides a 20 m thick pedosedimentary record of the last interglacial–glacial climatic cycle (Upper Pleistocene). Based on optical dating, a chronostratigraphy could be established for the last climatic cycle, yielding the first numerical ages of a loess record from the middle Danube basin. Infrared-stimulated luminescence (IR-OSL) dating has been applied to the polymineral silt fraction using a multiple aliquot additive-dose protocol to determine the equivalent dose (D_E). Within error limits, all age estimates are in stratigraphic order. Owing to the application of shine-plateau tests, the samples showed no evidence of insufficient bleaching. The Surduk loess section comprises three major periods of soil formation. Based on the IR-OSL chronostratigraphy, the lowermost pedocomplex is attributed to the Last Interglacial and to the Early Glacial (Marine Isotope Stage – MIS 5e to 5a). The middle part of the section exhibits a succession of weakly developed brown soils and a humic horizon, named 'Surduk soil', formed during MIS 3. On top of the section, recent soil formation is related to the Holocene. Thick loess deposits are preserved between these palaeosols and are attributed to the Lower and Upper Pleniglacials (MIS 4 and 2), respectively. Estimated mean sedimentation rates are 0.1–0.2 mm/yr for the last glacial cycle, with a strong increase to 0.6 mm/yr with onset of the Pleniglacial.

Markus Fuchs (e-mail: markus.fuchs@uni-bayreuth.de), Chair of Geomorphology, University of Bayreuth, D-95440 Bayreuth, Germany, Department of Geology, University of Cincinnati, PO Box 210013, Cincinnati, OH 45221-0013, USA. Denis-Didier Rousseau, Université de Montpellier II, Institut des Sciences de l'Evolution, UMR CNRS 5554, 34095 Montpellier cedex 05, France, Ecole Normale Supérieure de Paris, Laboratoire de Météorologie Dynamique, UMR CNRS 8539, 24 rue de Lhomond, 75231 Paris cedex 05, France, Lamont-Doherty Earth Observatory of Columbia University, Palisades, NY 10964, USA; Pierre Antoine, UMR CNRS 8591, Laboratoire de Géographyie Physique, 1 Place A. Briand, 92 195 Meudon France; Christine Hatté, Laboratoire des Sciences du Climat et de l'Environnement, UMR CNRS CEA 1572, avenue de la terrasse, 91198 Gif-sur-Yvette, France, NSF Arizona AMS Laboratory, Physics Building, P.O. Box 210081, Tucson, AZ 85721-0081, USA; Caroline Gauthier, Laboratoire des Sciences du Climat et de l'Environnement, UMR CNRS CEA 1572, avenue de la terrasse, 91198 Gif-sur-Yvette, France; Slobodan Marković, Chair of Physical Geography, Faculty of Sciences, University of Novi Sad, Trg Dositeja Obradovica 3, 21000 Novi Sad, Serbia; Ludwig Zoeller, Chair of Geomorphology, University of Bayreuth, D-95440 Bayreuth, Germany; *received 13th April 2007, accepted 13th August 2007.*

Loess–paleosol sequences represent one of the best terrestrial archives of past environmental and climatic conditions (e.g. Kukla 1977; Rousseau 1987; Hatté *et al*. 1998; Antoine *et al*. 2001; Rousseau *et al*. 2001; Haesaerts *et al*. 2003; Zöller *et al*. 2004). For southeast Europe, the loess deposits of the middle Danube basin are of great importance for reconstructing continental palaeoclimate (Marković-Marjanović 1969). In this context, numerous loess sections from the Vojvodina region in Serbia were recently investigated (e.g. Bronger *et al*. 1987; Bronger 2003; Marković *et al*. 2004, 2005, 2006, 2007), providing important information of Middle and Upper Pleistocene environmental change. However, for all the loess sections of this region, reliable numerical age estimates are still lacking (Frechen *et al*. 2003), hampering the possibility of adequate interpretation of the palaeoenvironmental archives. Furthermore, for the reconstruction of past climate conditions, various palaeoclimate records need to be correlated, which requires numerical age determinations.

To understand continental sedimentation processes, a chronology is fundamental. Luminescence dating techniques, which enable direct dating of the sediments and their last exposure to daylight (Aitken 1985), is the obvious technique and is widely used to establish numerical chronologies of loess deposits (e.g. Zöller *et al*. 1988; Frechen *et al*. 2003; Lang *et al*. 2003).

Recent research has focused on the impact of rapid climatic events and climate variability on European loess environments during the Last Glacial (e.g. Vandenberghe *et al*. 1998; Hatté *et al*. 1998; Antoine *et al*. 2001, 2003; Rousseau *et al*. 1998, 2001, 2002). As the Surduk section shows one of the best developed loess records of the last climatic cycle in the area, it is well suited for determination of the impact of rapid climatic changes using a multiproxy approach like stratigraphy, sedimentology, mollusc assemblages, geochemistry and IR-OSL dating techniques (Antoine *et al*. 2001, 2003; Rousseau *et al*. 2002).

In this study, we present for the first time a reliable chronostratigraphy from a loess section of the Vojvodina region in Serbia. The first TL dating results from the area were supplied by Singhvi *et al*. (1989), but they lacked a complete chronology of the last glacial cycle and, despite the keen approach to date loess older than the last glacial cycle, were still

DOI 10.1111/j.1502-3885.2007.00012.x

subject to age underestimation beyond *c*. 50 kyr (cf. Zöller *et al*. 1994). Infrared-stimulated luminescence (IR-OSL) dating techniques (Hütt *et al*. 1988) using polymineral silt were therefore applied in this study to establish a chronology for the last interglacial–glacial cycle.

Materials and methods

The Surduk loess section is situated on the right bank of the Danube river (45°4′N; 20°20′E, 111 m a.s.l.) in the southeastern Carpathian Basin, *c*. 30 km northwest of Belgrade, Serbia (Fig. 1).

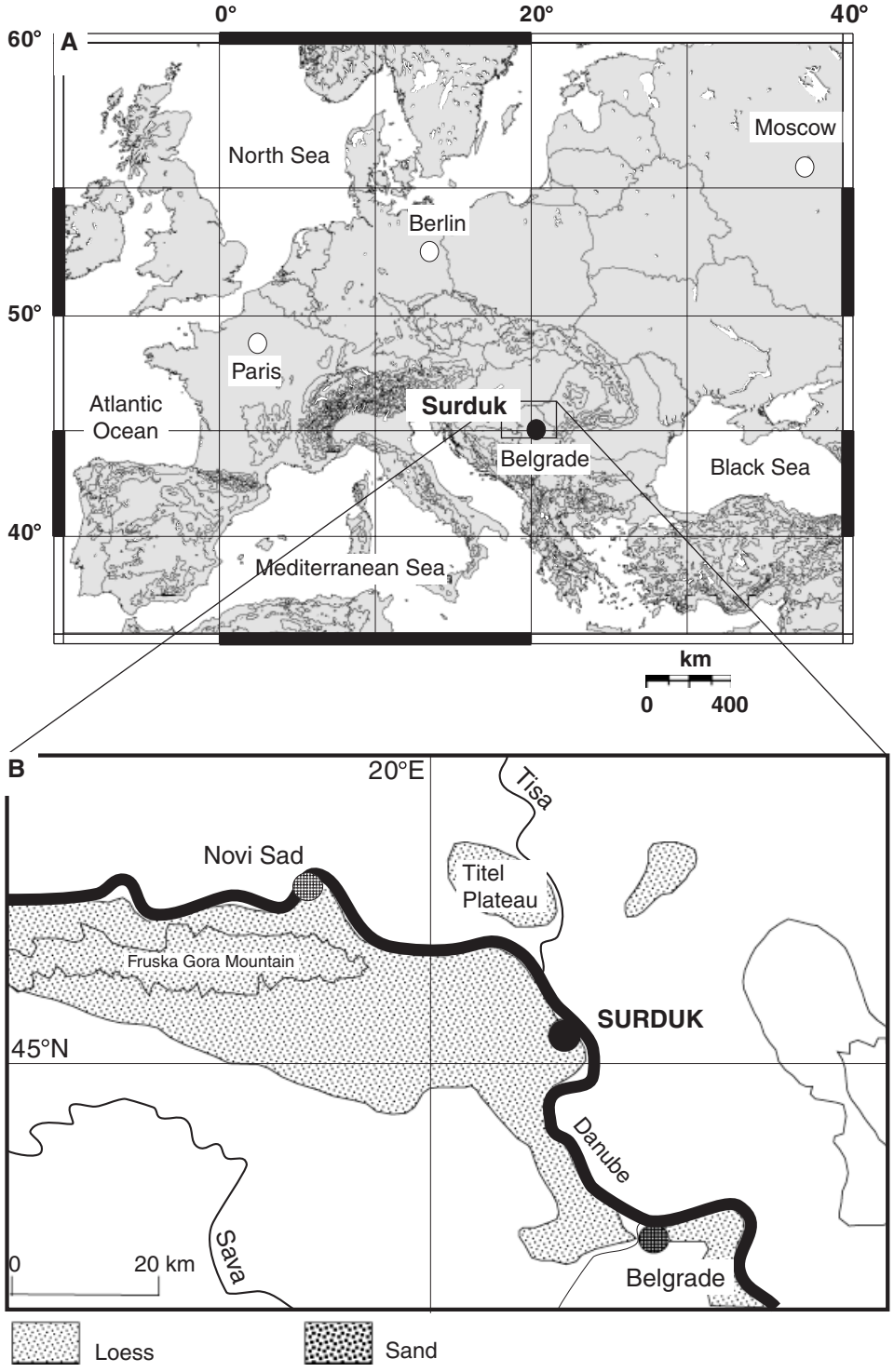

Fig. 1. Location of the Surduk loess section. A. Map showing the study area in Europe. B. Location of the Surduk sequence in the Vojvodina region in Serbia (from Markovic *et al*. 2004, modified).

Stratigraphy

Evidence of 14 sedimentary and pedological units could be identified within the 20 m thick loess profile (Fig. 2). The lower part of the section is characterized by a 2.3 m thick humic and clayey soil complex (units 13 and 12). The main part of this complex (unit 13) is composed of two superimposed Bth horizons of leached chernozem soils (Luvic Chernozem, FAO, 2006. Clay 26–33%; total organic content 0.4–0.6%) developed on the underlying calcareous loess (unit 14). The upper dark brown Ah humic horizon (unit 12) indicates a first step to more arid and cooler conditions. According to the pedological characteristics of this soil succession, and comparison with close loess sections studied in this region, which yielded amino acid geochronologies and correlations with other European loess series (Markovic *et al.* 2004, 2005, 2006), these soils are allocated to the Last Interglacial and Upper Pleistocene Early Glacial.

The onset of pure loess sedimentation is represented by 0.3 m of grey loess (unit 11), followed by deposition of a 2.8 m thick sandy loess with intercalated sandy layers (unit 10), which is allocated to the Lower Pleniglacial. This first pronounced period of aeolian sedimentation ends with the development of a new soil and sandy loess complex of 4.9 m thickness (units 9 to 4). This complex is composed of a succession of weak grey-brown Cambic horizons (units 9 and 7) separated by sandy loess units (units 5 and 8) and terminated by the formation of a 0.3 m thick humic horizon, named 'Surduk soil' (unit 4). This alternation of interstadial and stadial conditions represented by the alteration of loess and weakly developed soils has been observed and described in the northwestern European Middle Pleniglacial (e.g. Antoine *et al.* 2001), central and eastern European sequences (e.g. Kukla 1977; Veklitch 1979; Rousseau *et al.* 2001).

The upper 8 m of the profile is represented by typical loess deposits (Upper Pleniglacial), beginning with 2 m of brownish loess, which indicates intense biological activity. The section is topped by a reworked Chernozem horizon which is strongly altered by human activities, thus attributed to the Holocene.

The 20 m thick loess section is composed of three main periods of loess deposition (units 14, 10 and 2/3) separated by soil complexes. This pattern has been described in central (Stillfried B or PKII complexes; Kukla 1977) and eastern European (Vytachiv complex; Veklitch 1979, Rousseau *et al.* 2001) loess sequences. Within the Upper Pleistocene loess, the lower unit (10) is characterized by a distinct sand content and includes thin aeolian sand beds originating from the Danube alluvial plain. The upper loess units (2 and 3) are composed of typical homogeneous silty loess.

Low field magnetic susceptibility (MS)

The magnetic susceptibility was measured using a portable Bartington MF susceptibility meter. After carefully cleaning the section, the susceptibility was measured every 10 cm in the loess units and every 5 cm in the palaeosols (Fig. 2). An average value was calculated out of 10 readings per depth.

IR-OSL dating

Ten samples were taken for IR-OSL dating using cupper cylinders (ø 4 cm) hammered into the cleaned loess section to avoid any contamination of the samples with light-exposed material. Sample preparation was performed under subdued red light (640 ± 20 nm) using standard methods described by Lang *et al.* (1996). The polymineral fine-grain fraction (4–11 μm) was used for luminescence measurements.

To determine the equivalent dose (D_E), the multiple aliquot additive dose protocol was applied and data analysis was done with the Analyst software (Version 3.07b). In order to construct saturating exponential growth curves, 10 natural aliquots and 6 groups of artificially irradiated aliquots (5 each) were used. Artificial irradiation was performed with a $^{90}S/^{90}Y$ β-source (9.9 Gy/min). During IR stimulation ($880 \text{ nm} \pm 80$ nm), decay curves were measured for 60 s at room temperature after a preheat at 220 °C for 300 s and using a detection filter combination of BG39, $2 \times$ BG3 and GG400 (390–450 nm). After irradiation and before measurement, the samples were stored at room temperature for at least one month. Finally, the D_E was calculated from the 0–40 s signal integral after subtracting the 'late light' signal of the 50–60 s integral (Aitken & Xie 1992). All samples were checked for anomalous fading, using an additional set of natural and maximum dosed aliquots, with 10 aliquots for each sample. Irradiation and preheating of the fading-test aliquots were carried out contemporaneously to the irradiation and preheating of the aliquots for D_E determination, but were stored for a minimum of three months before measurements. Comparison of the ratios between the natural and the artificial irradiated intensities for the first and second measurements is used for the fading test. To determine the α-efficiency (a-value), three groups of artificially α-irradiated aliquots (three each) were used to construct the growth curve (^{241}Am α-source, 8.8 Gy/min). Dose rates ($\dot{D}$) were obtained using low-level γ-spectrometry and conversion factors given by Adamiec & Aitken (1998).

Results and discussion

The magnetic susceptibility (MS) shows values varying between $10.1 \times 10^{-8} \text{ m}^3 \text{ kg}^{-1}$ in the loess units and $90.7 \times 10^{-8} \text{ m}^3 \text{ kg}^{-1}$ in the soil complex at the base of the sequence (Fig. 2). The penultimate loess unit 14 shows low values of $c.$ $11 \times 10^{-8} \text{ m}^3 \text{ kg}^{-1}$, which increase regularly toward the top of subunit

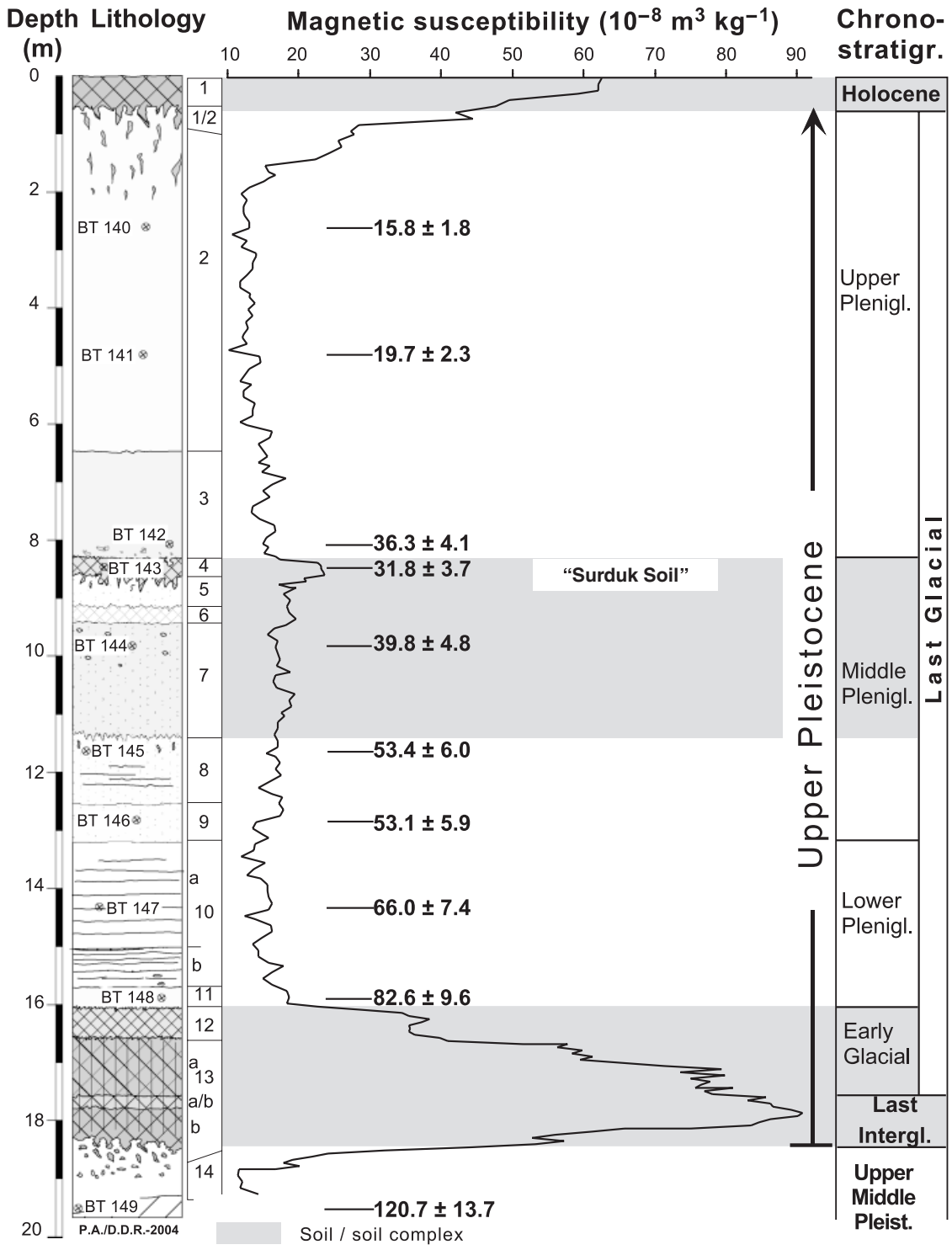

Fig. 2. Stratigraphy and low field magnetic susceptibility record of the Surduk loess section. Pedosedimentary units and sample locations for IR-OSL dating with their laboratory numbers and IR-OSL age estimates in kiloyears (kyr) are indicated. Unit description: 1 = Reworked Chernozem/top soil; 1/2 = Bioturbated horizon between top soil and underlying loess; 2 and 3 = Calcareous loess; 4 = Grey brown humic soil 'Surduk Soil'; 5 and 8 = Sandy loess with granular structure; 6 = Greyish weak humic horizon; 7 and 9 = Light brown sandy to clayey sandy silts (weakly developed Bw horizons); 10a = Sandy loess with numerous sand layers; 10b = Laminated sandy loess; 11 = Homogeneous light grey loess; 12 = Brown grey humic silt (Ah horizon/Chernozem soil); 13 = Dark brown clayey silt with aggregates and numerous biotubules (horizon of Chernozem); 13a/b = Greyish transitional horizon; 14 = Homogeneous calcareous loess.

Table 1. IR-OSL dating results.

Sample	Depth (m)	Δ	*a*-value	U (μm/g)	Th (μm/g)	K (%)	$\dot{D}$ (Gy/kyr)	D_E (Gy)	IR-OSL age (kyr)
BT 140	2.60	1.15 ± 0.1	0.05	3.05 ± 0.09	9.77 ± 0.46	1.41 ± 0.03	3.20 ± 0.32	50.41 ± 2.38	15.8 ± 1.8
BT 141	4.90	1.15 ± 0.1	0.10	3.36 ± 0.10	10.83 ± 0.49	1.44 ± 0.03	3.95 ± 0.42	77.80 ± 3.69	19.7 ± 2.3
BT 142	8.00	1.15 ± 0.1	0.08	3.52 ± 0.10	11.79 ± 0.52	1.57 ± 0.03	4.00 ± 0.42	145.19 ± 6.22	36.3 ± 4.1
BT 143	8.40	1.15 ± 0.1	0.05	3.49 ± 0.09	12.50 ± 0.52	1.58 ± 0.03	3.70 ± 0.38	117.49 ± 6.11	31.8 ± 3.7
BT 144	9.80	1.15 ± 0.1	0.07	3.67 ± 0.11	12.34 ± 0.55	1.61 ± 0.04	4.06 ± 0.43	161.56 ± 9.12	39.8 ± 4.8
BT 145	11.60	1.15 ± 0.1	0.06	3.19 ± 0.07	11.09 ± 0.40	1.57 ± 0.03	3.57 ± 0.37	190.60 ± 8.14	53.4 ± 6.0
BT 146	12.70	1.15 ± 0.1	0.06	3.12 ± 0.10	11.13 ± 0.53	1.58 ± 0.04	3.56 ± 0.37	188.80 ± 7.69	53.1 ± 5.9
BT 147	14.20	1.15 ± 0.1	0.06	3.38 ± 0.09	11.59 ± 0.49	1.67 ± 0.03	3.76 ± 0.39	247.90 ± 10.61	66.0 ± 7.4
BT 148	15.80	1.15 ± 0.1	0.06	3.53 ± 0.10	12.25 ± 0.54	1.70 ± 0.03	3.89 ± 0.41	321.46 ± 16.14	82.6 ± 9.6
BT 149	19.40	1.15 ± 0.1	0.06	2.99 ± 0.11	10.49 ± 0.56	1.38 ± 0.04	3.25 ± 0.34	391.90 ± 16.39	120.7 ± 13.7

Note: Δ = Water content given as the ratio of wet sample weight to dry sample weight; *a*-value = α-efficiency factor; U-, Th- and K-concentrations based on low-level γ-spectrometry (in none of the samples was significant radioactive disequilibrium present); U-concentrations calculated from ^{214}Bi and ^{214}Pb activities; $\dot{D}$ = effective dose rate; D_E = equivalent dose.

13b indicating the highest values. Subunits 13a/b and 13a show a decrease in the MS values in three different steps, at about $84.5 \times 10^{-8}\,m^3\,kg^{-1}$, $76.6 \times 10^{-8}\,m^3\,kg^{-1}$ and $60 \times 10^{-8}\,m^3\,kg^{-1}$. Unit 12 corresponds to another step in the decreasing trend of MS values (*c*. $35.9 \times 10^{-8}\,m^3\,kg^{-1}$), unit 11 corresponds to the last step ($18.8 \times 10^{-8}\,m^3\,kg^{-1}$) toward the minimum 'glacial' values. MS in the first Upper Pleistocene loess (units 10 to 5) is low, especially in the basal sandy unit (minimum of $14.4 \times 10^{-8}\,m^3\,kg^{-1}$). The Surduk soil (*c*. $22.9 \times 10^{-8}\,m^3\,kg^{-1}$) shows much lower values than in the basal pedocomplex or in the top soil. The upper loess, units 3 to 2, yield the lowest values (*c*. $10.1 \times 10^{-8}\,m^3\,kg^{-1}$) with an increasing trend on top of the series due to Holocene sediment contamination. The Holocene soil indicates an increasing trend from *c*. $28.5 \times 10^{-8}\,m^3\,kg^{-1}$ at the base to *c*. $62.5 \times 10^{-8}\,m^3\,kg^{-1}$ in the uppermost layer, the latter value remaining lower than in the basal soil complex owing to the modern erosion and reworking of the upper part of this soil.

Compared with the sediment succession, the MS record of Surduk shows a clear correlation between highest MS values and the main humic and clayey soil horizons as in units 12, 13 and 14 ('Surduk Soil'). This observation infers that the enrichment in magnetic minerals responsible for high MS values is linked to pedological processes, as proposed by several authors from Chinese loess sequences (Heller & Evans 1995; Sun & Huang 2006). This pedological enrichment in magnetic minerals (magnetite and maghemite) has been attributed to bacterial activity (magnetotactic bacteria) within soil horizons (Maher & Taylor 1988) and can be used as a proxy of palaeoprecipitation (Maher *et al*. 2003).

Apart from the record of the last interglacial and early glacial interval, the MS record shows similarities with measurements performed in both Dolni Vestonice, in the Czech Republic, and Vyazivok in Ukraine (Rousseau *et al*. 2001). In all sequences the two main aeolian deposits show very low values and bracket slightly higher measures corresponding to the intermediary soil complexes.

IR-OSL dating results including analytical data from $\dot{D}$ and D_E determination are listed in Table 1. None of the samples showed significant radioactive disequilibrium and no anomalous fading was detected after three months of storage, with general fading ratios between 0.9 and 1.1 ± 0.1, except for two samples (BT144, BT 149) with a fading ratio of 0.8 ± 0.2. The IR-OSL measurements were characterized by very good reproducibility. Shine-plateau tests applied to all samples resulted in constant D_E values for increasing integrals, which is an indication for sufficient bleaching. Examples from the IR-OSL measurements are given in Fig. 3.

IR-OSL ages are plotted in Fig. 3 with their stratigraphic information and according to sampling depth. The calculated ages represent an age range from 15.8 ± 1.8 kyr in the upper part of the section to 120.7 ± 13.7 kyr at its bottom. Within error limits, all age estimates are in stratigraphic order.

Sample BT 149 was taken from the calcareous loess of unit 14 below the main soil complex of units 12 and 13; providing an age of 120.7 ± 13.7 kyr, this is in agreement with an expected penultimate climatic cycle age. The ages obtained below and above the basal humic soil complex (unit 12/13) confirm its interpretation as the pedosedimentary budget of the Last Interglacial and of the first interstadials of the Upper Pleistocene (MIS 5e to 5a).

The lower Upper Pleistocene sandy loess sample BT 147 in the middle of unit 10 yields an age of 66.0 ± 7.4 kyr, but sedimentation of this lower sandy loess starts at 82.6 ± 9.6 kyr (BT 148) with unit 11 directly overlying the upper unit of the basal soil complex.

From the underlying sandy loess and interstadial soil complex (units 9 to 4) four IR-OSL ages were calculated. Two samples with ages of 53.1 ± 5.9 kyr (BT 146) in the lowermost incipient soil (unit 9) and 53.4 ± 6.0 kyr (BT 145) in the sandy loess of unit 8 followed by

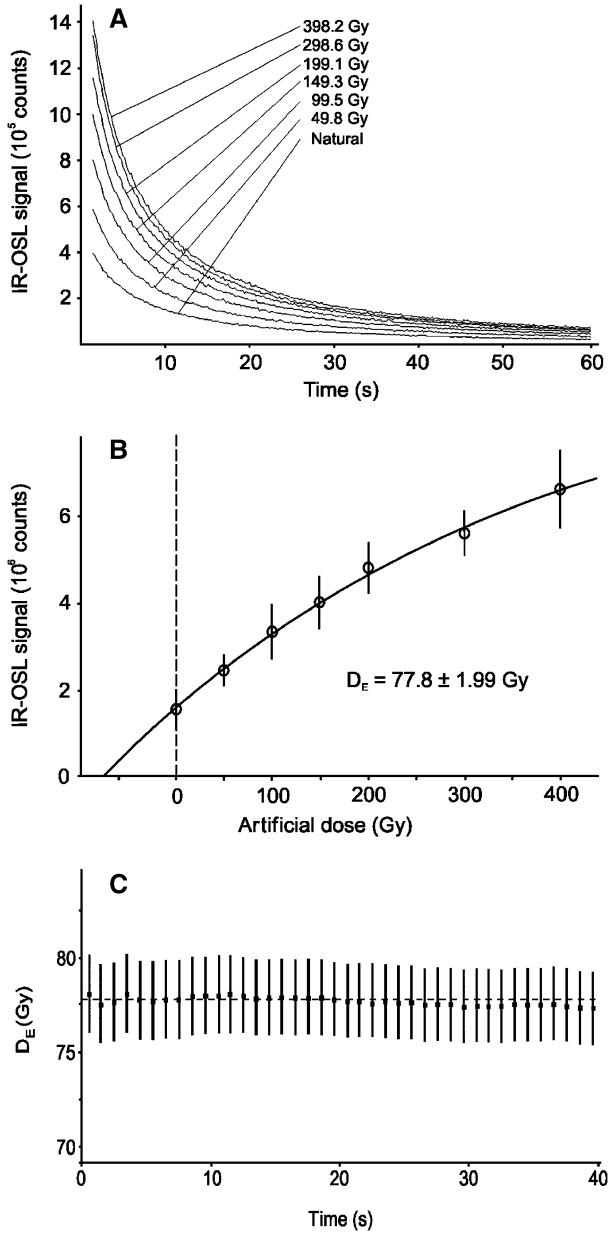

Fig. 3. IR-OSL measurement results of sample BT 141. A. Shine-down curves for the natural and artificial irradiated subsamples. Each curve represents the mean of 5–10 measurements. Additive doses are indicated. B. Saturating exponential growth curve with an estimated D_E of 77.8 ± 1.99 Gy. For D_E calculation, the integral from 0–40 s was used after subtracting the 'late light' signal from 50–60 s. C. D_E shine-plateau test for increasing integrals with a mean D_E represented by the broken line (77.8 ± 1.99 Gy). Constant D_E values over time indicate sufficient bleaching.

the uppermost sample (BT 144) from the weak brown soil of unit 7, which yields an age of 39.8 ± 4.8 kyr. The sediment from the humic 'Surduk soil' (unit 4) yields an age of 31.8 ± 3.7 kyr (BT 143). The entire loess and interstadial soil complex is therefore allocated to the Middle Pleniglacial (MIS 3).

The top 8.2 m of the section, defined as units 2 and 3, represents thick accumulations of loess. From these units, three IR-OSL ages could be determined. Sample BT 142 taken at the beginning of loess unit 3 indicates an age of 36.3 ± 4.1 kyr. At 3.9 m depth, sample BT 141 with an age of 19.7 ± 2.3 kyr represents the onset of pronounced loess accumulation during the Last Glacial Maximum. Sample BT 140 from 2.6 m depth yields an age of 15.8 ± 1.8 kyr, representing the end of the last Pleniglacial or onset of the Lateglacial.

Mean sedimentation rates can be estimated based on the calculated IR-OSL ages. Sedimentation rates of *c.* 0.1–0.2 mm/yr are characteristic of the basal humic soil complex up to onset of the Upper Pleniglacial around 20 kyr. This estimation of the sedimentation rate is based on seven calculations between the following IR-OSL ages: BT 149 to BT 148 (0.1 ± 0.04 mm/yr), BT 148 to BT 147 (0.1 ± 0.07 mm/yr), BT 147 to BT 146 (0.12 ± 0.08 mm/yr), BT 145 to BT 144 (0.13 ± 0.07 mm/yr), BT 144 to BT 143 (0.18 ± 0.12 mm/yr) and BT 142 to BT 141 (0.19 ± 0.05 mm/yr). No sedimentation rates could be calculated for mean age reversals between BT 146 to BT 145 and BT 143 to BT 142. It should be noted that these mean age reversals might represent high pulses of sedimentation. For the following period, especially for the youngest part of the Upper Pleniglacial, loess accumulation increases sharply to values of *c.* 0.6 mm/yr. This estimation is based on two values calculated for the time range between BT 142 and BT 141 (0.58 ± 0.4 mm/yr), and between BT 141 and the top of the profile (0.61 ± 0.02 mm/yr), with the top of the profile representing the end of loess accumulation at the Pleistocene/Holocene transition *c.* 11.5 kyr ago.

The sedimentation rates of 0.1–0.2 mm/yr for the lower section and 0.6 mm/yr for the upper section, which are based on individual calculations between samples, are confirmed by the slope of the correlation line from the data set of the lower and upper section. However, the given sedimentation rates are only mean values and can differ to much higher or lower values. The latter is true, for example, for periods of soil formation where sedimentation rates were assumed to be strongly reduced.

The highest sedimentation rates are obtained for the Upper Pleniglacial, a result similar to the general pattern described for all European series (Frechen *et al.* 2003; Haesaerts *et al.* 2003), and corresponding to the interval during which Greenland's atmosphere was the dustiest (GRIP Members 1993; Johnsen *et al.* 2001). This is also the interval during which high dilated aeolian material was deposited in the Rhine Valley, characterizing the occurrence of strong winds prevailing at both 45° and 50°N (Renssen & Bogaart 2003; Renssen & Vandenberghe 2003).

The chronostratigraphical framework defined in Surduk infers that the main change in the sedimentology, with the pedocomplex at the base and the aeolian sediments above, may correspond to the MIS 5/4 boundary at *c.* 75 kyr (Kukla & Briskin 1983;

Martinson *et al*. 1987). This boundary has already been documented in western, central and eastern European loess sequences (Antoine *et al*. 1999, 2001; Rousseau *et al*. 1998, 2001). Furthermore, the highest sedimentation rates observed in the Upper Pleniglacial imply that loess deposition in Europe was fairly homogeneous in terms of general timing. Such a uniform response over this large an area indicates major climatic shifts, though the transported material originated from various sources and varied from place to place due to regional context and conditions.

The similarity between the Surduk eolian sequence with other European sequences, located on a northern transect at about 50°N, indicates that they are all complete, especially since in all series weakly developed soils separate the two main loess sub-series. We then infer that units 10, 9 to 3, 2 to subunit 1/2 correspond to MIS 4, 3 and 2, respectively. Unit 1 corresponds to the Holocene, units 12 and 13 to MIS 5, and the penultimate loess, unit 14 to the top of MIS 6.

According to the stratigraphy, high-resolution grain-size analysis, MS and organic carbon analysis and IR-OSL chronology, the Surduk loess section yields one of the most detailed dated environment and climate changes during the last interglacial–glacial climatic cycle in the south southeastern Carpathian basin.

Conclusions

IR-OSL dating of the Surduk loess section demonstrates its excellent suitability for establishing high resolution chronologies. Within error limits, the calculated ages are in stratigraphic order, comprising the last interglacial–glacial cycle, and reinforce the chronostratigraphical interpretation of the pedosedimentary sequence. Estimated sedimentation rates show a strong increase during the younger part of the Upper Pleniglacial, confirming results obtained from loess regions in central Europe (Lang *et al*. 2003; Frechen *et al*. 2003). Based on the given chronostratigraphy and in combination with further investigations on palaeoclimatic proxies from the high resolution continuous sampling (grain size, organic carbon $\delta^{13}C$, molluscs, etc.), a complete palaeoclimate interpretation of the Surduk loess section is in progress.

Acknowledgements. – This is contributions ISEM 2007-074, LDEO-7058, LSCE-2347. The study was funded through the CNRS ECLIPSE programme and the French-Serbian Pavle Savic exchange programme. Many thanks to Manfred Fischer of the University of Bayreuth for IRSL sample preparation.

References

Adamiec, G. & Aitken, M. 1998: Dose-rate conversion factors: Update. *Ancient TL 16*, 37–50.

Aitken, M. 1985: *Thermoluminescence Dating*. 359 pp. Academic Press, London.

Aitken, M. & Xie, J. 1992: Optical dating: Recuperation after bleaching. *Quaternary Science Reviews 11*, 147–152.

Antoine, P., Rousseau, D.-D., Hatté, C., Zöller, L., Lang, A., Fontugne, M. & Moine, O. 2003: Événements éoliens rapides en contexte loessique: l'exemple de la séquence du Pléniglaciaire supérieur weichselien de Nussloch (Vallée du Rhin-Allemagne). *Quaternaire 13*, 199–208.

Antoine, P., Rousseau, D.-D., Lautridou, J. P. & Hatté, C. 1999: Last Interglacial–Glacial climatic cycle in loess-paleosol successions of north-western France. *Boreas 28*, 551–563.

Antoine, P., Rousseau, D.-D., Zöller, L., Lang, A., Munaut, A. V., Hatté, C. & Fontugne, M. 2001: High-resolution record of the last interglacial–glacial cycle in the Nussloch loess palaeosol sequences, Upper Rhine Area, Germany. *Quaternary International 76–77*, 211–229.

Bronger, A. 2003: Correlation of loess–paleosol sequences in East and Central Asia with SE Central Europe: towards a continental Quaternary pedostratigraphy and paleoclimatic history. *Quaternary International 106/107*, 11–31.

Bronger, A., Pant, R. K. & Singhvi, A. K. 1987: Micromorphology, mineralogy, genesis and dating of loess-paleosol sequences and their application to Pleistocene chronostratigraphy and paleoclimate: A comparison between Southeast Central Europe and the Kashmir Valley/Central Asia. In Tungsheng, L. (ed.): *Aspect of Loess Research*, 121–129. China-Ocean-Press, Beijing.

FAO, 2006: *World Reference Base for Soil Resources: FAO World Soil Resource Reports 103*, 145 pp. Rome.

Frechen, M., Oches, E. A. & Kohfeld, K. E. 2003: Loess in Europe – mass accumulation rates during the Last Glacial Period. *Quaternary Science Reviews 22*, 1835–1857.

GRIP Members 1993: Climate instability during the last interglacial period recorded in the GRIP ice core. *Nature 364*, 203–207.

Haesaerts, P., Borziak, I., Chirica, V., Damblon, F., Koulakovska, L. & van der Plicht, J. 2003: The east Carpathian loess record: A reference for the Middle and Late Pleniglacial stratigraphy in central Europe. *Quaternaire 14*, 163–188.

Hatté, C., Fontugne, M., Rousseau, D.-D., Antoine, P., Zöller, L., Tisnerat-Laborde, N. & Bentaleb, I. 1998: $\delta^{13}C$ variations of loess organic matter as a record of the vegetation response to climatic changes during the Weichselian. *Geology 26*, 583–586.

Heller, F. & Evans, M. E. 1995: Loess magnetism. *Reviews of Geophysics 33*, 211–240.

Hütt, G., Jaek, I. & Tchonka, J. 1988: Optical dating: K-feldspars optical response stimulation spectra. *Quaternary Science Reviews 7*, 381–385.

Johnsen, S. J., Dahl-Jensen, D., Gundestrup, N., Steffensen, J. P., Clausen, H. B., Miller, H., Masson-Delmotte, V., Sveinbjörnsdottir, A. E. & White, J. 2001: Oxygen isotope and palaeotemperature records from six Greenland ice-core stations: Camp Century, Dye-3, GRIP, GISP2, Renland and NorthGRIP. *Journal of Quaternary Science 16*, 299–307.

Kukla, G. 1977: Pleistocene land–sea correlations. 1. Europe. *Earth-Science Reviews 13*, 307–374.

Kukla, G. & Briskin, M. 1983: The age of the 4/5 isotopic stage boundary on land and in the oceans. *Palaeogeography, Palaeoclimatology, Palaeoecology 42*, 35–45.

Lang, A., Hatté, C., Rousseau, D.-D., Antoine, P., Fontugne, M., Zöller, L. & Hambach, U. 2003: High-resolution chronologies for loess: Comparing AMS ^{14}C and optical dating results. *Quaternary Science Reviews 22*, 953–959.

Lang, A., Lindauer, S., Kuhn, R. & Wagner, G. A. 1996: Procedures used for optical and infrared stimulated dating of sediments in Heidelberg. *Ancient TL 14*, 7–11.

Maher, B. A., Alekseeva, A. & Alekseevab, T. 2003: Magnetic mineralogy of soils across the Russian Steppe: Climatic dependence of pedogenic magnetite formation. *Palaeogeography, Palaeoclimatology, Palaeoecology 201*, 321–341.

Maher, B. A. & Taylor, R. M. 1988: Formation of ultrafine-grained magnetite in soils. *Nature 336*, 368–370.

Marković-Marjanović, J. 1969: Les profils de loess du Bassin pannonique. Région classique du loess en Yougoslavie. *Bulletin de l'Association Française pour l'Etude du Quaternaire* 165–170.

Marković, S., Kostić, N. & Oches, E. A. 2004: Paleosols in the Ruma loess section (Vojvodina, Serbia). *Revista Mexicana de Ciencias Geologicas 21*, 79–87.

Marković, S. B., Bokhorst, M., Vandenberghe, J., McCoy, W. D., Oches, E. A., Hambach, U., Gaudenyi, T., Jovanović, M., Zöller, L., Stevens, T. & Machalett, B. 2007: Late Pleistocene loess-paleosol sequences in the Vojvodina region, North Serbia. *Journal of Quaternary Science*, doi: 10.1002/jqs.1124.

Marković, S. B., McCoy, W. D., Oches, E. A., Savić, S., Gaudenyi, T., Jovanović, M., Stevens, T., Walther, R., Ivanisević, P. & Galić, Z. 2005: Paleoclimate record in the Upper Pleistocene loess–paleosol sequence at Petrovaradin brickyard (Vojvodina, Serbia). *Geologica Carpathica 56*, 545–552.

Marković, S. B., Oches, E. A., Sümegi, P., Jovanović, M. & Gaudenyi, T. 2006: An introduction to the Middle and Upper Pleistocene loess–paleosol sequence at Ruma brickyard, Vojvodina, Serbia. *Quaternary International 149*, 80–86.

Martinson, D., Pisias, M. G., Hays, J. D., Imbrie, J., Moore, T. C. & Shackleton, N. J. 1987: Age dating and the orbital theory of ice ages: Development of a high-resolution 0 to 300,000-year chronostratigraphy. *Quaternary Research 27*, 1–29.

Renssen, H. & Bogaart, P. W. 2003: Atmospheric variability over the ~14.7 kyr BP stadial–interstadial transition in the North Atlantic region as simulated by an AGCM. *Climate Dynamics 20*, 301–313.

Renssen, H. & Vandenberghe, J. 2003: Investigation of the relationship between permafrost distribution in NW Europe and extensive winter sea-ice cover in the North Atlantic Ocean during the cold phases of the Last Glaciation. *Quaternary Science Reviews 22*, 209–223.

Rousseau, D.-D. 1987: Paleoclimatology of the Achenheim series (middle and upper Pleistocene, Alsace, France). A malacological analysis. *Palaeogeography, Palaeoclimatology, Palaeoecology 59*, 293–314.

Rousseau, D.-D., Antoine, P., Hatté, C., Lang, A., Zöller, L., Fontugne, M., Ben Othman, D., Luck, J.-M., Moine, O., Labonne, M., Bentaleb, I. & Jolly, D. 2002: Abrupt millennial climatic changes from Nussloch (Germany) Upper Weichselian eolian records during the Last Glaciation. *Quaternary Science Reviews 21*, 1577–1582.

Rousseau, D.-D., Gerasimaenko, N., Matvviishina, Z. & Kukla, G. J. 2001: Late Pleistocene environments of the Central Ukraine. *Quaternary Research 56*, 349–356.

Rousseau, D.-D., Zöller, L. & Valet, J. P. 1998: Climatic variations in the Upper Pleistocene loess sequence at Achenheim (Alsace, France). Based on a magnetic susceptibility TL chronology of loess. *Quaternary Research 49*, 255–263.

Singhvi, A. K., Bronger, A., Sauer, W. & Pant, R. K. 1989: Thermoluminescence dating of loess–paleosol sequences in the Carpathian Basin: A suggestion for a revised chronology. *Chemical Geology 73*, 307.

Sun, J. & Huang, X. 2006: Half-precessional cycles recorded in Chinese loess: Response to low-latitude insolation forcing during the Last Interglaciation. *Quaternary Science Reviews 25*, 1065–1072.

Vandenberghe, J., Huijzer, B., Mücher, H. & Laan, W. 1998: Short climatic oscillations in a western European loess sequence (Kesselt, Belgium). *Journal of Quaternary Science 13*, 471–485.

Veklitch, M. F. 1979: Pleistocene loesses and fossil soils of the Ukraine. *Acta Geologica Scientiarum Hungaricae 22*, 35–62.

Zöller, L., Oches, E. A. & McCoy, W. D. 1994: Towards a revised chronostratigraphy of loess in Austria with respect to key sections in the Czech Republic and in Hungary. *Quaternary Geochronology (Quaternary Science Reviews) 13*, 465–472.

Zöller, L., Rousseau, D.-D., Jäger, K. D. & Kukla, G. 2004: Last interglacial, Lower and Middle Weichselian – a comparative study from the Upper Rhine and Thuringian loess areas. *Zeitschrift für Geomorphologie N.F. 48*, 1–24.

Zöller, L., Stremme, H. E. & Wagner, G. A. 1988: Thermolumineszenz-Datierung an Löß-Paläoboden-Sequenzen von Nieder-, Mittel- und Oberrhein. *Chemical Geology 73*, 39–62.